



## Molecular states of prednisolone dispersed in folded sheet mesoporous silica (FSM-16)

Akinori Nishiwaki<sup>a</sup>, Aya Watanabe<sup>a</sup>, Kenjirou Higashi<sup>a</sup>, Yuichi Tozuka<sup>b</sup>,  
Kunikazu Moribe<sup>a</sup>, Keiji Yamamoto<sup>a,\*</sup>

<sup>a</sup> Graduate School of Pharmaceutical Sciences, Chiba University, 1-33 Yayoi-cho, Inage-ku, Chiba 263-8522, Japan

<sup>b</sup> Gifu Pharmaceutical University, 5-6-1, Mitahora-higashi, Gifu 502-8585, Japan

### ARTICLE INFO

#### Article history:

Received 17 December 2008

Received in revised form 14 May 2009

Accepted 16 May 2009

Available online 22 May 2009

#### Keywords:

Solid dispersion

Folded sheet mesoporous material

Molecular interaction

Solid-state NMR

Prednisolone

### ABSTRACT

Modes of molecular interaction between prednisolone and mesoporous materials have been investigated by the technique of solid-state NMR. Folded sheet mesoporous material (FSM-16) was used as host material and prednisolone was used as guest molecule. A suspension of FSM-16 in prednisolone dichloromethane solution was evaporated to prepare the evaporated samples. <sup>13</sup>C NMR spectroscopy was used as well as powder X-ray diffractometry and differential scanning calorimetry. Crystalline behavior of prednisolone disappeared in the evaporated samples, indicating the monomolecular dispersion of prednisolone in FSM-16 matrices. NMR peak shifts and broadening could be attributed to the molecular interaction between the A ring of prednisolone and FSM-16. Thermal properties of prednisolone were investigated after heat treatment of the evaporated samples. The results indicated that the thermal stability of the dispersion made from FSM-16 of large pore size was superior to that from FSM-16 of small pore size. Hydrocortisone was used to compare the dispersion state with prednisolone. It was suggested that the double bond at the C-1 and C-2 positions of prednisolone might play an important role in the process of adsorption of prednisolone to FSM-16.

© 2009 Published by Elsevier B.V.

### 1. Introduction

It is known that bioavailability is correlated with *in vitro* dissolution behavior when a water-insoluble drug is administered orally. Improving the dissolution of a drug has become an important topic in pharmaceutical studies. To improve dissolution, use of inclusion compounds (Arima et al., 1996; Hirayama et al., 1996) and solvate (Sekiguchi et al., 1973), expansion of crystal surface area by size reduction (Chattopadhyay and Gupta, 2001) and use of polymorphic forms with excellent solubility (Kobayashi et al., 2000) have been applied.

A method using a porous substance that has minute holes in its structure changes the drug to an amorphous material. When a porous powder that has large relative surface area with minute-hole structure was mixed with crystals that can be sublimed, it was confirmed that the drug was taken up into the minute holes through the vapor phase at normal temperature, which is different from the study this time in terms of drug absorption by solvent evaporation and also it was confirmed that it existed not as a crystal but as a solid dispersion (Tozuka et al., 2003). Moreover, it was reported that the dissolution rate of a drug that has been adsorbed

to porous powder was better than that of a drug that exists as single crystals (Oguchi et al., 1997). Therefore, some research in recent years has attempted to improve physical properties by adsorbing the drug in porous powder to improve the dissolution of the drug (Salonen et al., 2005; Takeuchi et al., 2005). Control of dissolution behavior has not been successful completely since it is difficult to know the status regarding adsorption of the drug in a sample. However, there are several attempts to investigate drug loading to mesoporous materials and releasing from them (Andersson et al., 2004; Heikkilä et al., 2007; Mellaerts et al., 2007, 2008; Vallet-Regí et al., 2007).

Powder X-ray diffractometry, infra-red spectroscopy, differential scanning calorimetry, etc. are analytical methods that have been used for evaluation of the molecules of drugs that exist in minute holes in porous powder. Information regarding the degree of crystallization, molecular interactions, and thermal behavior is obtained by these methods, respectively. However, there are limits in the information obtained because, using the powder X-ray diffractometry, no peak arises from crystals in the solid dispersion of an amorphous solid and an endothermic peak from melting hardly appears even in the differential scanning calorimetry (Leuner and Dressman, 2000).

Solid-state NMR spectroscopy is a technique that recently began to be used for the evaluation of physical properties of solid drugs (Berendt et al., 2006; Nelson et al., 2006). In addition to being a

\* Corresponding author. Tel.: +81 43 290 2938; fax: +81 43 290 2939.  
E-mail address: [yamamotok@p.chiba-u.ac.jp](mailto:yamamotok@p.chiba-u.ac.jp) (K. Yamamoto).

nondestructive measurement, the features of solid-state NMR spectroscopy are that the obtained information is accumulated from individual atomic nuclei and that the chemical shift of the signal given by the individual atomic nucleus is influenced only from the extremely local magnetic environment. Therefore, even if the drug is an amorphous solid or a mixture, the adsorption of its molecules can be selectively measured at the nano level. Moreover, it is reported that some information regarding conformation and mobility of the molecule in the solid state is obtained by measurement of relaxation time in solid-state NMR spectroscopy and a linear analysis. It is also reported that solid-state NMR spectroscopy has been used for quantitative analysis and structure analysis of drugs (Babonneau et al., 2004; Lubach et al., 2004; Park et al., 2005; Sheth et al., 2005; Xu and Harris, 2005; Aso and Yoshioka, 2006; Azaïs et al., 2006; Barich et al., 2006; Harris et al., 2006; Masuda et al., 2006; Farrer et al., 2007; Nunes et al., 2007). Various examinations, including characterization and quantitation of crystal polymorphism, evaluation of mobility for guest compounds in the amylose complex and investigation, using PVP and SDS, of the mechanism regarding formation of nano particles of a drug, have been done in our laboratory (Tozuka et al., 2002, 2006; Pongpeerapat et al., 2006).

Folded sheet mesoporous material (FSM-16) has been prepared by an intercalation of quarterly ammonium surfactant as a template in a layered sodium silicate, kanemite, followed by calcination to remove the template (Kresge et al., 1992; Inagaki et al., 1996; Dapaah et al., 1999). FSM-16 shows high specific surface area such as 1000 m<sup>2</sup>/g and narrow pore size distribution in the meso range of 2–50 nm. FSM-16 has honeycomb one-dimensional straight channels, and it shows excellent heat resistance and pressure resistance (Inaki et al., 2000; Cassiers et al., 2002; Matsumoto et al., 2002).

We studied mode of interaction between the drug and FSM-16 by solid-state NMR spectroscopy. The technique has been used to investigate the interaction between benzoic acid and FSM-16 (Tozuka et al., 2005). An advantage of solid-state NMR spectroscopy is that the study can be focused only on the drug since all the peaks observed are derived from the drug. This is because FSM-16 is a porous silica material which is composed of only silicon, oxygen and hydrogen and does not contain carbon. FSM-16 (Oc) whose mean pore diameter was 16.0 Å and FSM-16 (Do) whose mean pore diameter was 21.6 Å were used to investigate the interaction between the size of the pores in the silica material and the characteristic of the drug. Prednisolone, one of the steroids, was used as a model compound since it is water-insoluble and is not sublimed. Hydrocortisone was also used to investigate molecules of a drug that has a different steroid structure than prednisolone.

## 2. Materials and methods

### 2.1. Materials

Folded sheet mesoporous material-16 (FSM-16) was provided by Toyota Central R&D Labs, Inc., Japan. Two FSM-16 of different pore sizes, which was measured by N<sub>2</sub> adsorption, were used. They were FSM-16 (Oc) which has a mean pore diameter of 16.0 Å and FSM-16 (Do) which has a mean pore diameter of 21.6 Å. Specific surface areas are 700 m<sup>2</sup>/g (FSM-16 (Oc)) and 1250 m<sup>2</sup>/g (FSM-16 (Do)), respectively. “Oc” represents n-octyltrimethyl ammonium bromide (or chloride) and “Do” represents n-dodecyltrimethyl ammonium bromide (or chloride). A pore size changes depending on the molecular size of surfactants used. FSM-16 was slightly ground and sieved to less than 125 μm and dried under reduced pressure at 110 °C for 3 h. Prednisolone (stable form) was supplied by Sigma–Aldrich Japan. Metastable form prednisolone was prepared by the evaporation of prednisolone dichloromethane solution. Hydrocortisone

was supplied by Nacalai Tesque, Japan. Dichloromethane was used as a reagent grade.

### 2.2. Preparation of physical mixture (PM)

FSM-16 and steroid were physically mixed in a glass vial using a vortex mixer for 1 min to prepare PM. The concentration of steroid in each sample was 30% by weight.

### 2.3. Preparation of evaporated sample (EVP)

Ninety milligram of steroid was dissolved in dichloromethane and then 210 mg of FSM-16 was added. The mixture was sonicated for 3 min. Dichloromethane was removed by a rotary evaporator to obtain EVP. The concentration of steroid in each sample was 30% by weight.

### 2.4. Preparation of sealed heated sample (EVP-SH)

Three hundred milligrams of EVP was sealed in a glass ampoule (27 mL volume) and heated at 140 °C for 3 h to obtain EVP-SH. 140 °C was chosen as a heating temperature to identify any change in experiments with less amount of decomposed products.

### 2.5. Powder X-ray diffractometry (PXRD)

Measurement of PXRD was carried out using Rigaku Miniflex CN2005B111. Powder sample was applied on a glass plate so that the surface of the powder was flat. Conditions of measurement were Cu Kα radiation, scanning speed: 4°/min and scanning angle: 2–35°.

### 2.6. Differential scanning calorimetry (DSC)

DSC was performed using SII Nano Technology EXSTAR6000 DSC6200. Each sample was measured in a crimped aluminum pan under N<sub>2</sub> gas (60 mL/min) with heating rate of 5 °C/min. The calibration was done by using indium.

### 2.7. Solid-state nuclear magnetic resonance (NMR) spectroscopy

All <sup>13</sup>C solid-state NMR spectra were acquired using JNM-ECA600 NMR spectrometer that had a magnetic field of 14.09 T (JEOL, Japan) operating at 150 MHz for <sup>13</sup>C. Samples (ca. 100 mg) were placed as powders into 4 mm silicon nitride (Si<sub>3</sub>N<sub>4</sub>) rotors. <sup>13</sup>C spectra were acquired using variable amplitude cross-polarization (CP) together with magic angle spinning (MAS) at 15 kHz and a high-power two-pulse phase-modulation <sup>1</sup>H decoupling. For each spectrum, total number of accumulations (1000–30000) was acquired depending on the signal-to-noise ratio required. Pertinent acquisition parameters included relaxation delays of 3 s for all experiments, a CP contact time of 5 ms and a <sup>1</sup>H 90° pulse of 2.7 μs. The total number of data points was 2048 points per spectrum in each experiment and zero-filled to 8192 points. All spectra were externally referenced to tetramethylsilane by setting the higher field peak of adamantane to 29.5 ppm. Carbon spin–lattice relaxation times (T<sub>1</sub>) were measured by monitoring the recovery of <sup>13</sup>C magnetization following cross-polarization and inversion (Torchia, 1978). Values of T<sub>1</sub> were determined from the initial rates of this recovery.

## 3. Results and discussion

### 3.1. Molecular state of prednisolone in FSM-16

As the two-dimensional molecular size of prednisolone was evaluated as 9.8 Å × 13.7 Å from the consideration based on van der

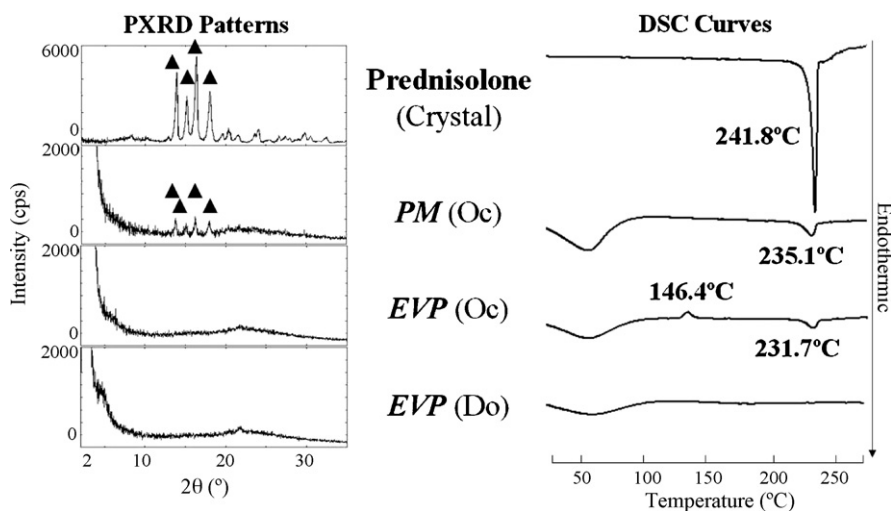


**Fig. 1.** PXRD patterns and DSC curves of physical mixture [PM (Oc)] and evaporated samples with FSM-16 (Oc) [EVP (Oc)] and evaporated sample with FSM-16 (Do) [EVP (Do)].

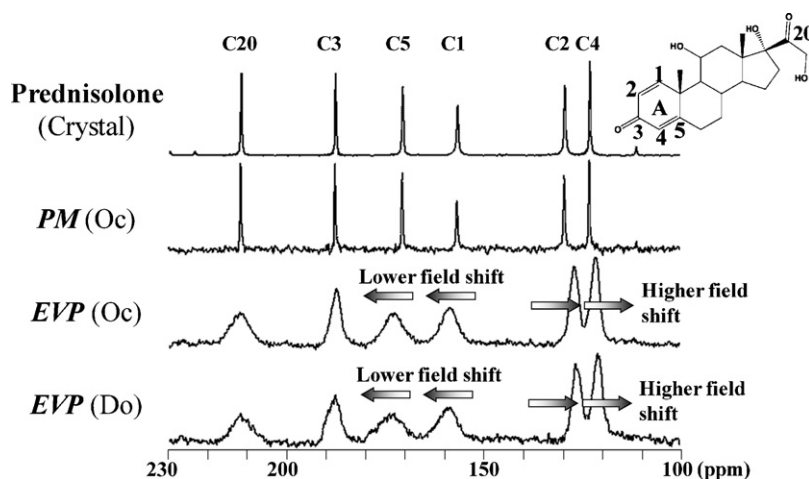
Waals radius, a prednisolone molecule could theoretically fit to the pore size of FSM-16 where the pore diameter of FSM-16 (Oc) and FSM-16 (Do) were 16.0 and 21.6 Å, respectively.

Fig. 1 represents the PXRD patterns and DSC curves of prednisolone stable form, the physical mixture with FSM-16 (Oc) [PM (Oc)], the evaporated sample with FSM-16 (Oc) [EVP (Oc)] and the evaporated sample with FSM-16 (Do) [EVP (Do)]. Black triangles in the PXRD patterns demonstrate X-ray diffraction peaks of prednisolone crystals. PM (Oc) showed an X-ray diffraction pattern similar to that of prednisolone crystals, as FSM-16 was an amorphous material. The pattern of PM (Do) was in good agreement with that of PM (Oc). Regarding the two evaporated samples, the pattern changed to halo pattern and clear diffraction peaks were not observed. These results indicated that most of the prednisolone molecules were transformed to amorphous form during the evaporation process, and presumably they existed within the pores of FSM-16.

In the DSC curve of prednisolone crystals, a melting endothermic peak was observed at around 242 °C, and with PM as well. A small exothermic peak at about 140 °C was found in the evaporated sample with FSM-16 (Oc). This peak was supposed to be due to the crystallization of prednisolone during the heating process. No characteristic thermal event was observed for EVP (Do). This suggested that the pore size of FSM-16 affected the stability of the dispersed

state of prednisolone in the dispersion matrix. Results of PXRD patterns and DSC curves indicated that prednisolone adsorbed to either FSM-16 (Oc) or FSM-16 (Do) after evaporation.

Fig. 2 shows  $^{13}\text{C}$  NMR spectra of the solid dispersion samples in the range of 100–230 ppm. All the NMR peaks originated from carbon atoms of prednisolone since FSM-16 has no carbon atoms. The  $^{13}\text{C}$  NMR spectrum of PM was very similar to the carbon resonance of prednisolone crystals. The peak positions in evaporated samples with both FSM-16 (Oc) and (Do), however, were shifted and their peak shapes became broad. A newly-formed intermolecular interaction such as hydrogen bonding has been reported to affect the chemical environment of the neighboring molecules, causing chemical shifts to downfield or upfield (Kuo and Chang, 2001; Shenderovich et al., 2003). The NMR peak shifts were mainly observed on the carbon atoms of the A ring of prednisolone. It was suggested that the formation of new hydrogen bonding between carbonyl group (C3) of prednisolone and the hydroxyl group of FSM-16 induced the changes of the conjugated double bond system of the A ring in prednisolone. Mollica et al. (2006) reported that line broadening of  $^{13}\text{C}$  CP/MAS NMR peaks were a result of a larger distribution of isotropic chemical shifts, arising from wider distribution of chemical environments for the same carbons belonging to different drug molecules. Broad NMR peaks detected in the evaporated samples indicated that the prednisolone molecules with a broader



**Fig. 2.**  $^{13}\text{C}$  CP/MAS spectra of physical mixture [PM (Oc)] and evaporated samples with FSM-16 (Oc) [EVP (Oc)] and evaporated sample with FSM-16 (Do) [EVP (Do)].

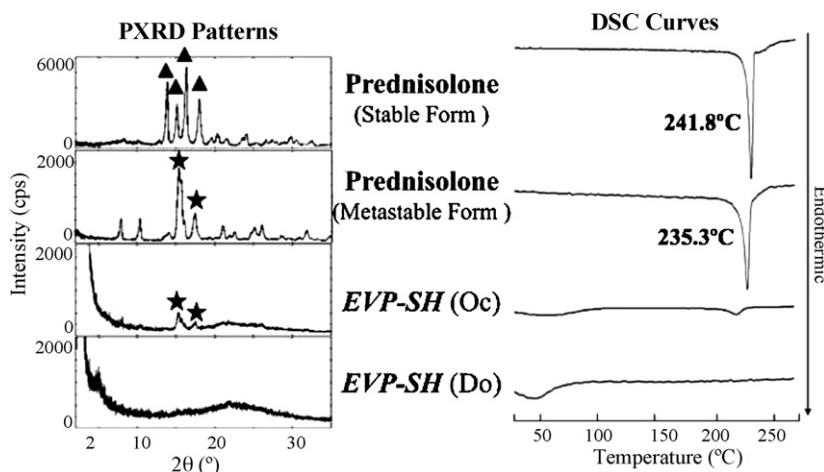


Fig. 3. PXRD patterns and DSC curves of prednisolones and sealed heated samples with FSM-16 (Oc) [EVP-SH (Oc)] and with FSM-16 (Do) [EVP-SH (Do)].

conformational distribution, which suggested higher molecular mobility, were present in the matrix.  $^{13}\text{C}$  NMR spectra as well as PXRD patterns and DSC curves suggested that prednisolone was adsorbed as amorphous form to FSM-16.  $T_1$  value for each  $^{13}\text{C}$  signal of prednisolone was determined by using Torchia's methods to evaluate the molecular mobility. Each  $^{13}\text{C}$  signal of prednisolone in PM showed longer  $T_1$  values ( $>300$  s), while that in EVP showed shorter one ( $<50$  s). (Accurate  $T_1$  values could not be obtained for the EVP samples because of the broader peak and poor sensitivity.) Smaller  $T_1$  values imply more enhanced molecular motion for the solid-state samples (Yang et al., 2006; Takahashi et al., 2004). It was indicated that molecular mobility of prednisolone in EVP samples was much more enhanced due to the interaction with FSM-16.

### 3.2. Relationship between physical stability of dispersion state and pore size of FSM-16

The sealed heated samples were used to clarify the thermal stability of amorphous state in the dispersion matrix. Fig. 3 presents the PXRD patterns and DSC curves of prednisolone stable form, prednisolone metastable form, the sealed heated sample of EVP-16 (Oc) [EVP-SH (Oc)] and the sealed heated sample of EVP-16 (Do) [EVP-SH (Do)]. Small X-ray diffraction peaks were observed in EVP-SH (Oc), which were identical to the peaks of prednisolone metastable form (star symbols), while no X-ray diffraction peaks were detected in the EVP-SH (Do). In EVP-SH (Oc), prednisolone partly existed in the metastable form outside of the pores. Prednisolone which was not able to stay in the pore of FSM-16 (Oc) was crystallized while heating process even though the prednisolone had been captured in the FSM-16 (Oc). A surface condition of the FSM-16 (Oc) related to crystallization as the metastable form since the formation of crystal depends on where the crystallization occurs. In EVP-SH (Do), prednisolone still existed in the amorphous dispersed state in the pores of FSM-16 (Do). This was also confirmed by the DSC measurements. A small melting peak was observed in the EVP-SH (Oc) and there was no peak with EVP-SH (Do). The pore size of FSM-16 (Do) is larger than that of FSM-16 (Oc), and the larger pore size of FSM-16 contributed to the thermal stability of dispersion state.

Fig. 4 represents  $^{13}\text{C}$  NMR spectra of sealed heated samples observed in the range of 100–230 ppm. The sealed heated sample with FSM-16 (Oc) showed sharp resonances. The observed chemical shift was in fair agreement with that of the prednisolone metastable form. The sealed heated sample of EVP-16 (Do) showed broad signals, which was similar to that of EVP (Do). This suggested that prednisolone molecules had been adsorbed to FSM-16 (Do) pores even after sealed heating process. It was found that the amorphous

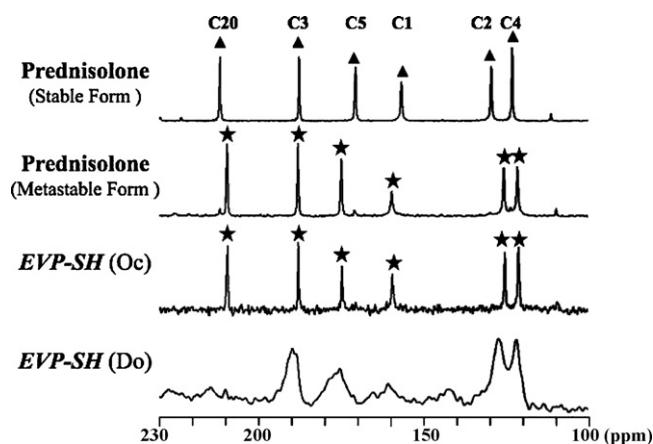


Fig. 4.  $^{13}\text{C}$  CP/MAS NMR spectra of prednisolones and sealed heated samples with FSM-16 (Oc) [EVP-SH (Oc)] and with FSM-16 (Do) [EVP-SH (Do)].

stability of prednisolone depended on the difference of the FSM pore size and that the larger size of pores contributed to high heat stability.

### 3.3. Comparison of molecular state of prednisolone with hydrocortisone

As the interaction between the A ring of prednisolone and FSM-16 was suggested, we investigated the effect of chemical structure

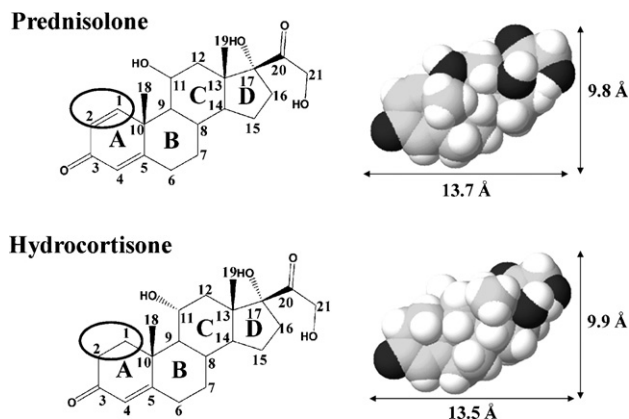
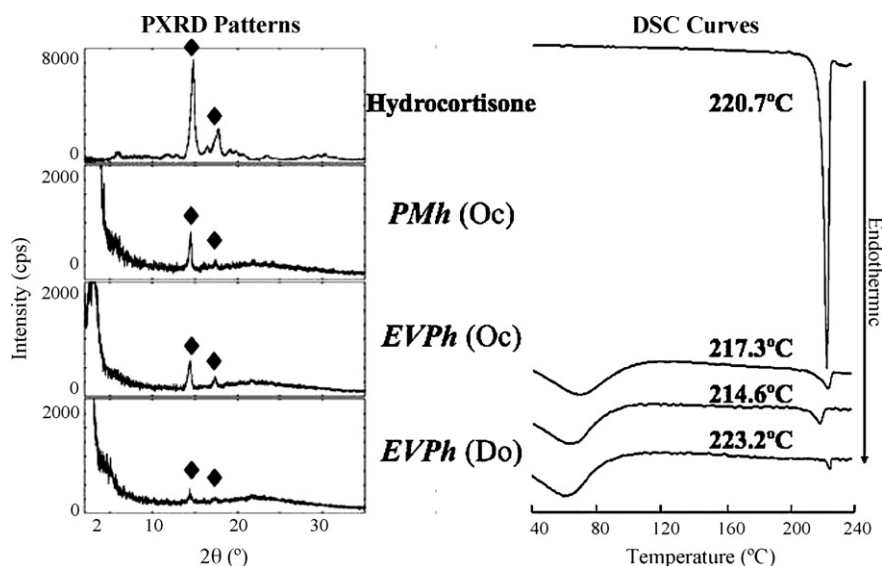


Fig. 5. Molecular structure of prednisolone and hydrocortisone.





**Fig. 6.** PXRD patterns and DSC curves of physical mixture [PMh (Oc)] and evaporated samples with FSM-16 (Oc) [EVPh (Oc)] and evaporated sample with FSM-16 (Do) [EVPh (Do)].

of guest molecule on the dispersibility in the matrix. Hydrocortisone was selected as a different guest molecule for FSM-16. The molecular structure of hydrocortisone is the same as that of prednisolone except the double bond at C1 and C2 positions, which is shown in Fig. 5. The double bond at C1–C2 position enhances glucocorticoid activity like anti-inflammatory effect (hydrocortisone vs. prednisolone = 1 vs. 4) and it reduces mineralocorticoid activity like sodium retention (hydrocortisone vs. prednisolone = 1 vs. 0.8).

Evaporated samples with hydrocortisone were prepared. Fig. 6 represents the PXRD patterns and DSC curves of hydrocortisone crystals, the physical mixture with FSM-16 (Oc) [PMh (Oc)], the evaporated sample with FSM-16 (Oc) [EVPh (Oc)] and the evaporated sample with FSM-16 (Do) [EVPh (Do)]. Diamond symbols represent X-ray diffraction peaks of hydrocortisone crystals. With regard to PXRD patterns, PMh and EVPh (Oc) had identical diffraction peaks with hydrocortisone. In the evaporated sample with FSM-16 (Do), the peak intensities were smaller than those of evaporated sample with EVPh (Oc). With respect to DSC curves, there was the same trend as with PXRD patterns. This is due to an intrinsic difference of compounds between prednisolone and hydrocortisone. The reason why there is still some crystalline behavior in the large pore material is thought to be that FSM-16 (Do) does not have enough pore size to have it as an amorphous since its molecular size is large. It is considered that there would not be any

crystalline behavior if we use the larger pore size of FSM-16 than FSM-16 (Do).

Fig. 7 demonstrates  $^{13}\text{C}$  NMR spectra of the evaporated samples with hydrocortisone. In the spectrum of hydrocortisone crystals, sharp peaks were due to carbon atoms of the 3, 4, 5 and 20 positions of hydrocortisone. The spectrum of the evaporated sample with FSM-16 (Oc) was similar to that of hydrocortisone crystals, while the evaporated sample with FSM-16 (Do) showed comparatively broad peaks. These results suggested that hydrocortisone molecules did not adsorb to the FSM-16 (Oc) pore structure and that some hydrocortisone could adsorb to FSM-16 (Do) as an amorphous state in the pores. The different results between hydrocortisone and prednisolone in  $^{13}\text{C}$  NMR spectra were assumed to be due to the difference of the double bond at C1–C2 position.

#### 4. Conclusion

PXRD patterns, DSC curves and  $^{13}\text{C}$  CP/MAS NMR spectra revealed that the molecular state of prednisolone changed from crystal state to amorphous state during the evaporation method with FSM-16. Thermal properties of prednisolone in FSM-16 depended on the pore size of FSM-16. In the dispersion with large pore size FSM-16, prednisolone molecules existed stably even in the heating process, while they crystallized during heating from the dispersion of small pore size FSM. Comparison of prednisolone with hydrocortisone suggested that the double bond at the C-1 and C-2 position of prednisolone was critical for the adsorption of steroid to FSM-16. It was found that the larger size of pore contributed to the heat stability of the drugs.

#### Acknowledgment

The authors are grateful to The Uehara Memorial Foundation for financial support of this work.

#### References

- Andersson, J., Rosenholm, J., Areva, S., Lindén, M., 2004. Influences of material characteristics on ibuprofen drug loading and release profiles from ordered micro- and mesoporous silica matrices. *Chem. Mater.* 16, 4160–4167.
- Arima, H., Miyaji, T., Irie, T., Hirayama, F., Uekama, K., 1996. Possible enhancing mechanism of the cutaneous permeation of 4-biphenylacetic acid by  $\beta$ -cyclodextrin derivatives in hydrophilic ointment. *Chem. Pharm. Bull.* 44, 582–586.

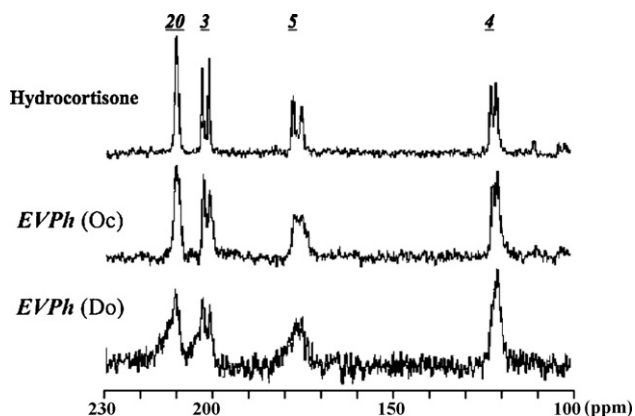


**Fig. 7.**  $^{13}\text{C}$  CP/MAS spectra of hydrocortisone evaporated samples with FSM-16 (Oc) [EVPh (Oc)] and evaporated sample with FSM-16 (Do) [EVPh (Do)].

- Aso, Y., Yoshioka, S., 2006. Molecular mobility of nifedipine–PVP and phenobarbital–PVP solid dispersions as measured by  $^{13}\text{C}$ -NMR spin–lattice relaxation time. *J. Pharm. Sci.* 95, 318–325.
- Azaïs, T., Tourné-Péteilh, C., Aussenac, F., Baccile, N., Coelho, C., Devoisselle, J.M., Babonneau, F., 2006. Solid-state NMR study of ibuprofen confined in MCM-41 material. *Chem. Mater.* 18, 6382–6390.
- Babonneau, F., Yeung, L., Steunou, N., Gervais, C., Ramila, A., Vallet-Regi, M., 2004. Solid-state NMR characterisation of encapsulated molecules in mesoporous silica. *J. Sol–Gel Sci. Technol.* 31, 219–223.
- Barich, D.H., Davis, J.M., Schieber, L.J., Zell, M.T., Munson, E.J., 2006. Investigation of solid-state NMR line widths of ibuprofen in drug formulations. *J. Pharm. Sci.* 95, 1586–1594.
- Berendt, R.T., Sperger, D.M., Isbester, P.K., Munson, E.J., 2006. Solid-state NMR spectroscopy in pharmaceutical research and analysis. *Trends Anal. Chem.* 25, 977–984.
- Cassiers, K., Linssen, T., Mathieu, M., Benjelloun, M., Schrijnemakers, K., van der Voort, P., Cool, P., Vansant, E.F., 2002. A detailed study of thermal, hydrothermal, and mechanical stabilities of a wide range of surfactant assembled mesoporous silicas. *Chem. Mater.* 14, 2317–2324.
- Chattopadhyay, P., Gupta, R.B., 2001. Production of griseofulvin nanoparticles using supercritical  $\text{CO}_2$  antisolvent with enhanced mass transfer. *Int. J. Pharm.* 228, 19–31.
- Dapaah, J.K.A., Uemichi, Y., Ayame, A., Matsuhashi, H., Sugioka, M., 1999. Activity enhancement of mesoporous silica (FSM-16) by modification with iron (II) sulphate for the isomerization of 1-butene. *Appl. Catal.* 187, 107–113.
- Farrer, B.T., Peresypkin, A., Wenslow, R.M., 2007. Quantitation of crystalline material within a liquid vehicle using  $^1\text{H}/^{19}\text{F}$  CP/MAS NMR. *J. Pharm. Sci.* 96, 264–267.
- Harris, R.K., Joyce, S.A., Pickard, C.J., Cadars, S., Emsley, L., 2006. Assigning carbon- $^{13}\text{C}$  NMR spectra to crystal structures by the inadequate pulse sequence and first principles computation: a case study of two forms of testosterone. *Phys. Chem. Chem. Phys.* 8, 137–143.
- Heikkilä, T., Salonen, J., Tuura, J., Kumar, N., Salmi, T., Murzin, D.Y., Hamdy, M.S., Mul, G., Laitinen, L., Kaukonen, A.M., Hirvonen, J., Lehto, V.-P., 2007. Evaluation of mesoporous TCPSi, MCM-41, SBA-15, and TUD-1 materials as API carriers for oral drug delivery. *Drug Deliv.* 14, 337–347.
- Hirayama, F., Minami, K., Uekama, K., 1996. In-vitro evaluation of biphenyl acetic acid- $\beta$ -cyclodextrin conjugates as colon-targeting prodrugs: drug release behaviour in rat biological media. *J. Pharm. Pharmacol.* 48, 27–31.
- Inagaki, S., Koiwai, A., Suzuki, N., Fukushima, Y., Kuroda, K., 1996. Syntheses of highly ordered mesoporous materials, FSM-16, derived from kanemite. *Bull. Chem. Soc. Jpn.* 69, 1449–1457.
- Inaki, Y., Yoshida, H., Kimura, K., Inagaki, S., Fukushima, Y., Hattori, T., 2000. Photometathesis activity and thermal stability of two types of mesoporous silica materials, FSM-16 and MCM-41. *Phys. Chem. Chem. Phys.* 2, 5293–5297.
- Kobayashi, Y., Ito, S., Itai, S., Yamamoto, K., 2000. Physicochemical properties and bioavailability of carbamazepine polymorphs and hydrate. *Int. J. Pharm.* 193, 137–146.
- Kresge, C.T., Leonowicz, M.E., Roth, W.J., Vartuli, J.C., Beck, J.S., 1992. Ordered mesoporous molecular sieves synthesized by a liquid-crystal template mechanism. *Nature* 359, 710–712.
- Kuo, S.W., Chang, F.C., 2001. Studies of miscibility behavior and hydrogen bonding in blends of poly(vinylphenol) and poly(vinylpyrrolidone). *Macromolecules* 34, 5224–5228.
- Lubach, J.W., Padden, B.E., Winslow, S.L., Salsbury, J.S., Masters, D.B., Topp, E.M., Munson, E.J., 2004. Solid-state NMR studies of pharmaceutical solids in polymer matrices. *Anal. Bioanal. Chem.* 378, 1504–1510.
- Leuner, C., Dressman, J., 2000. Improving drug solubility for oral delivery using solid dispersions. *Eur. J. Pharm. Biopharm.* 50, 47–60.
- Masuda, K., Tabata, S., Kono, H., Sakata, Y., Hayase, T., Yonemochi, E., Terada, K., 2006. Solid-state  $^{13}\text{C}$  NMR study of indomethacin polymorphism. *Int. J. Pharm.* 318, 146–153.
- Matsumoto, A., Sasaki, T., Nishimiya, N., Tsutsumi, K., 2002. Thermal stability and hydrophobicity of mesoporous silica FSM-16. *Colloids Surf. A: Physicochem. Eng. Aspects* 203, 185–193.
- Mellaerts, R., Aerts, C.A., Humbeek, J.V., Augustijns, P., Mooter, G.V., Martens, J.A., 2007. Enhanced release of itraconazole from ordered mesoporous SBA-15 silica materials. *Chem. Commun.* 13, 1375–1377.
- Mellaerts, R., Jammaer, J.A.G., Speybroeck, M.V., Chen, H., Humbeek, J.V., Augustijns, P., Mooter, G.V., Martens, J.A., 2008. Physical state of poorly water soluble therapeutic molecules loaded into SBA-15 ordered mesoporous silica carriers: a case study with itraconazole and ibuprofen. *Langmuir* 24, 8651–8659.
- Mollica, G., Geppi, M., Pignatello, R., Veracini, Carlo, A., 2006. Molecular properties of flurobiprofen and its solid dispersions with Eudragit RL100 studied by high- and low-resolution solid-state nuclear magnetic resonance. *Pharm. Res.* 23, 2129–2140.
- Nelson, B.N., Schieber, L.J., Barich, D.H., Lubach, J.W., Offerdahl, T.J., Lewis, D.H., Heinrich, J.P., Munson, E.J., 2006. Multiple-sample probe for solid-state NMR studies of pharmaceuticals. *Solid State Nucl. Magn. Reson.* 29, 204–213.
- Nunes, C.D., Vaz, P.D., Fernandes, A.C., Ferreira, P., Romão, C.C., Calhorda, M.J., 2007. Loading and delivery of sertraline using inorganic micro and mesoporous materials. *Eur. J. Pharm. Biopharm.* 66, 357–365.
- Oguchi, T., Tozuka, Y., Okonogi, S., Yonemochi, E., Oguchi, T., Yamamoto, K., 1997. Improved dissolution of naproxen from solid dispersions with porous additives. *Yakuzaigaku* 57, 168–173.
- Park, J.S., Kang, H.W., Park, S.J., Kim, C.K., 2005. Use of CP/MAS solid-state NMR for the characterization of solvate molecules within estradiol crystal forms. *Eur. J. Pharm. Biopharm.* 60, 407–412.
- Pongpeerapat, A., Higashi, K., Tozuka, Y., Moribe, K., Yamamoto, K., 2006. Molecular interaction among probucol/PVP/SDS multicomponent system investigated by solid-state NMR. *Pharm. Res.* 23, 2566–2574.
- Salonen, J., Laitinen, L., Kaukonen, A.M., Tuura, J., Björkqvist, M., Heikkilä, T., Vähä-Heikkilä, K., Hirvonen, J., Lehto, V.P., 2005. Mesoporous silicon microparticles for oral drug delivery: loading and release of five model drugs. *J. Control. Rel.* 108, 362–374.
- Sekiguchi, K., Kanke, M., Tsuda, Y., Ishida, K., Tsuda, T., 1973. Dissolution behavior of solid drugs. III. Determination of the transition temperature between the hydrate and anhydrous forms of phenobarbital by measuring their dissolution rates. *Chem. Pharm. Bull.* 21, 1592–1600.
- Shenderovich, I.G., Buntkowsky, G., Schreiber, A., Gedat, E., Sharif, S., Albrecht, J., Golubev, N.S., Findenegg, G.H., Limbach, H., 2003. Pyridine- $^{15}\text{N}$ —a mobile NMR sensor for surface acidity and surface defects of mesoporous silica. *J. Phys. Chem. B* 107, 11924–11939.
- Sheth, A.R., Lubach, J.W., Munson, E.J., Muller, F.X., Grant, D.J.W., 2005. Mechanochromism of piroxicam accompanied by intermolecular proton transfer probed by spectroscopic methods and solid-phase changes. *J. Am. Chem. Soc.* 127, 6641–6651.
- Takahashi, K., Yamamoto, H., Onoda, A., Doi, M., Inaba, T., Chiba, M., Kobayashi, A., Taguchi, T., Okamura, T., Ueyama, N., 2004. Highly oriented aragonite nanocrystal–biopolymer composites in an aragonite brick of the nacreous layer of *Pinctada fucata*. *Chem. Commun.*, 996–997.
- Takeuchi, H., Nagira, S., Yamamoto, H., Kawashima, Y., 2005. Solid dispersion particles of amorphous indomethacin with fine porous silica particles by using spray-drying method. *Int. J. Pharm.* 293, 155–164.
- Torchia, D.A., 1978. The measurement of proton-enhanced carbon- $^{13}\text{C}$   $T_1$  values by a method which suppresses artifacts. *J. Magn. Reson.* 30, 613–616.
- Tozuka, Y., Ito, A., Seki, H., Oguchi, T., Yamamoto, K., 2002. Characterization and quantitation of clarithromycin polymorphs by powder X-ray diffractometry and solid-state NMR spectroscopy. *Chem. Pharm. Bull.* 50, 1128–1130.
- Tozuka, Y., Oguchi, T., Yamamoto, K., 2003. Adsorption and entrapment of salicylamide molecules into the mesoporous structure of folded sheets mesoporous material (FSM-16). *Pharm. Res.* 20, 926–930.
- Tozuka, Y., Sasaoka, S., Nagae, A., Moribe, K., Oguchi, T., Yamamoto, K., 2005. Rapid adsorption and entrapment of benzoic acid molecules onto mesoporous silica (FSM-16). *J. Colloid Interface Sci.* 291, 471–476.
- Tozuka, Y., Takeshita, A., Nagae, A., Wongmekiat, A., Moribe, K., Oguchi, T., Yamamoto, K., 2006. Specific inclusion mode of guest compounds in the amylose complex analyzed by solid state NMR spectroscopy. *Chem. Pharm. Bull.* 54, 1097–1101.
- Vallet-Regí, M., Balas, F., Arcos, D., 2007. Mesoporous materials for drug delivery. *Angew. Chem. Int. Ed.* 46, 7548–7558.
- Xu, M., Harris, K.D.M., 2005. Altering the polymorphic product distribution in a solid-state dehydration process by rapid sample rotation in a solid-state NMR probe. *J. Am. Chem. Soc.* 127, 10832–10833.
- Yang, H., Hu, S., Horii, F., Endo, R., Hayashi, T., 2006. CP/MAS  $^{13}\text{C}$  NMR analysis of the structure and hydrogen bonding of melt-crystallized poly(vinyl alcohol) films. *Polymer* 47, 1995–2000.